



DREAMERS

Design REsearch, implementation And Monitoring of Emerging technologies for a new generation of Resilient Steel buildings

Report on the advanced FE studies quantifying the robustness of the demonstrator building

Deliverable D4.5-WP4-T4.5

WP 4: Advanced experimental tests. Development of advanced FE analyses for the dissemination activities.

<u>Task 4.5 – Advanced Robustness analyses with structural and non-structural</u> elements

Coordinator:

University of Liege

Authors:

Tudor Golea, Jean-Marc Franssen & Jean-François Demonceau

University of Liege, Belgium









Universidade de Coimbra









Date: 02.07.2024

Contents

LIST	OF FIGURES	2
LIST	OF TABLES	3
1. I	ntroduction	4
2. <i>A</i>	Assumed accidental scenarios	4
3. §	Structural model	5
3.1.	GLOBAL MODELLING ASSUMPTIONS	5
3.2.	MODELLING OF FREEDAM JOINTS	6
3.2.1. 3.2.2.	SIMPLIFIED TWO-SPRING MODEL MODEL VALIDATION	6 7
4.	Structural robustness under column loss scenarios	. 13
4.1. 4.1.1. 4.1.2.	STRUCTURAL ROBUSTNESS UNDER PERIMETER COLUMN LOSS SCENARIO ROBUSTNESS OF THE BARE STEEL STRUCTURE (BSS) ROBUSTNESS CONTRIBUTION OF NON-STRUCTURAL FAÇADE ELEMENTS	13 13 15
4.2.	STRUCTURAL ROBUSTNESS UNDER CORNER COLUMN LOSS SCENARIO	18
4.3.	STRUCTURAL ROBUSTNESS UNDER INTERNAL COLUMN LOSS SCENARIO	19
5. (Conclusions	. 20
REF	ERENCES	. 22

LIST OF FIGURES

Figure 1. Plane view of the DREAMERS building floor - Assumed base floor colun scenarios	
Figure 2. Material constitutive law	5
Figure 3. Slab diaphragm effect modelling	5
Figure 4. FREEDAM joint modelling	7
Figure 5. Extraction location of the analysed joint	7
Figure 6. Schematic view of the numerical model – Test 1	8
Figure 7. Simplified 2SM validation – Test 1	8
Figure 8. Predicted moment vs. rotation curves – Test 1	9
Figure 9. Schematic view of the numerical model – Test 2	10
Figure 10. Beam axial force vs. lateral support horizontal displacement	10
Figure 11. Applied force vs. vertical displacement curves	11
Figure 12. Beam axial force vs. vertical displacement curves	11
Figure 13. Connection moment vs. rotation curves	12
Figure 14. Behaviour laws for the assembly of components active at the damper level.	13
Figure 15. Column loss loading sequence	13
Figure 16. BSS response under the perimeter column loss (Scenario 1)	14
Figure 17. Internal forces acting on the FREDAM joint	14
Figure 18. M-N evolution in the 1 st floor joints of the DAP	15
Figure 19. Evolution of forces in the 2SM for joints at the extremities of the DAP	15
Figure 20. Fragility curves for façade walls with enhanced connections subjected to d loads (Landolfo et al. (2019))	
Figure 21. Fragility curves for façade walls with enhanced connections subjected to d loads (Landolfo et al. (2019))	
Figure 22. Schematical view of façade panels integration in the FE model	17
Figure 23. Column axial force vs. displacement further to the perimeter column loss	17
Figure 24. Structural response under the corner column loss (Scenario 2)	18
Figure 25. Structural response under the internal column loss (Scenario 3)	19
Figure 26. Evolution of tensile forces in the beams of the DAP	19
Figure 27. Structural response under the internal column loss	20

LIST	$\Gamma \cap$	FΤ	ΔΡ	I F	2
டு	u	г .	AD		

1. Introduction

Although the tying method is normatively prescribed for the design for robustness of all structures in consequences class 2, the achieved level of structural robustness remains uncertain. The application of this design method can be seen as a minimum but not necessarily sufficient requirement. Moreover, the analytical formulae for determining the tying resistance demand are not endorsed by a solid scientific background, which raises doubts about the method's applicability and reliability. Therefore, the use of more advanced procedures such as the standard-prescribed "notional removal of supporting elements" approach, also known as the alternative load path approach, requiring the consideration of geometrical and material non-linearities, is justified for any structure with significant consequences of failure. The requirement to be met is to prove that, upon the removal of any supporting column (or beam supporting a column), the stability of the structure is not affected, and the extent of local damages remains under specific limits. Since the loss of a supporting member can be caused by a multitude of accidental events, this approach allows assessing the robustness of a structure regardless of the accidental action that triggers the member loss, thus covering a wide range of unidentifiable accidental actions. As recommended by EN 1991-1-7, when the loss of a member leads to a progressive collapse or the local damage associated to the member loss exceeds the predefined limits, the design should turn towards methods of local enhancement of resistance and ductility of the member under consideration. The application of this method to the DREAMERS building will be considered with a specific attention paid to the influence of non-structural elements.

2. Assumed accidental scenarios

Given the variety of accidental actions that can lead to a column loss (e.g., fire, explosions, impacts), the latter can be treated as a dynamic or quasi-static event. As stated in the FAILNOMORE design manual (Demonceau et al., 2021), EN 1991-1-7 which deals with the design for robustness is not stating if this notional column removal has to be assumed as instantaneous, i.e. as "dynamic", or as "quasi-static". The consideration of a "quasi-static" removal allows (i) the use of more simple tools as no dynamic effects need to be accounted for and (ii) to have a good indication on the ability of a structure to activate alternative load paths. Hereinafter, considering that the DREAMERS building is included in CC2, lower risk group, the structural behaviour upon the loss of supporting columns will be analysed under quasi-static conditions.

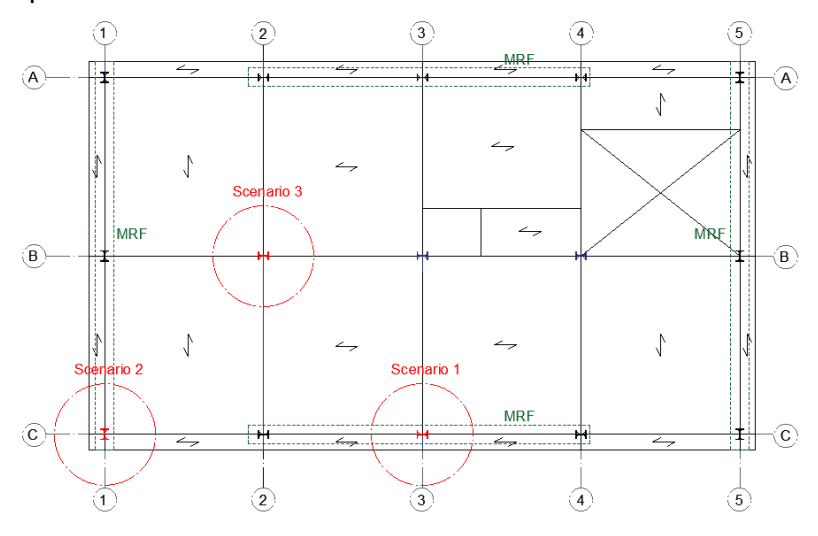


Figure 1. Plane view of the DREAMERS building floor - Assumed base floor column loss scenarios

Three distinct scenarios were chosen for investigating the structural robustness further to a column loss. As depicted in Figure 1, an internal column loss is assumed, which allows evaluating the level

of tensile forces reached in the hinged beams provided in the inner bays of the structure further to the column loss. The other two scenarios concern perimeter and corner column losses and highlight the influence of the local behaviour of the FREEDAM joints on the overall response and robustness of the DREAMERS building.

3. Structural model

3.1. Global modelling assumptions

The column loss was numerically simulated through nonlinear static analyses in the homemade finite element software FINELG. The software allows performing different types of analyses (e.g., elastic, nonlinear, static/dynamic) with account for geometric and material nonlinearities.

The structural model was built using classical 3D beam elements (7 degrees of freedom) with material behaviour laws incorporating the yielding plateau and the strain hardening of steel material. The provisions of the new draft of prEN 1993-1-14 (2021) were used to define the nonlinear behaviour law for the S355 steel as illustrated in Figure 2.

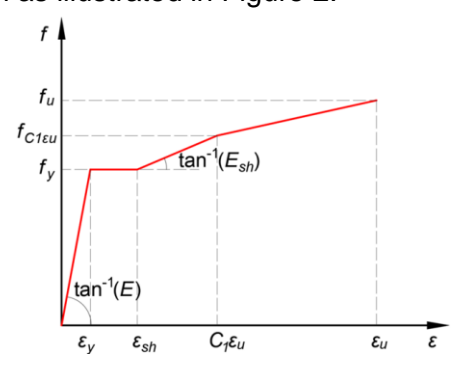


Figure 2. Material constitutive law

The composite slab consisting of Cofradal 260 floor solution was not explicitly modelled. However, given the importance of the slab contribution to the structural response under lateral loads due to the diaphragm effect, the latter was considered through a horizontal bracing system at the level of each floor as illustrated in Figure 3 (highlighted in red) and as recommended in the FAILNOMORE design manual. Rigid beam elements with circular cross-section were used to model the bracing elements such that the relative horizontal displacements between the columns at the level of each slab are prevented, thus simulating the rigid diaphragm provided by the slabs. This modelling approach generally leads to conservative results when column loss scenarios are considered since the slab contribution to the floor plastic mechanism and the possible activation of membrane action within the slab are neglected.

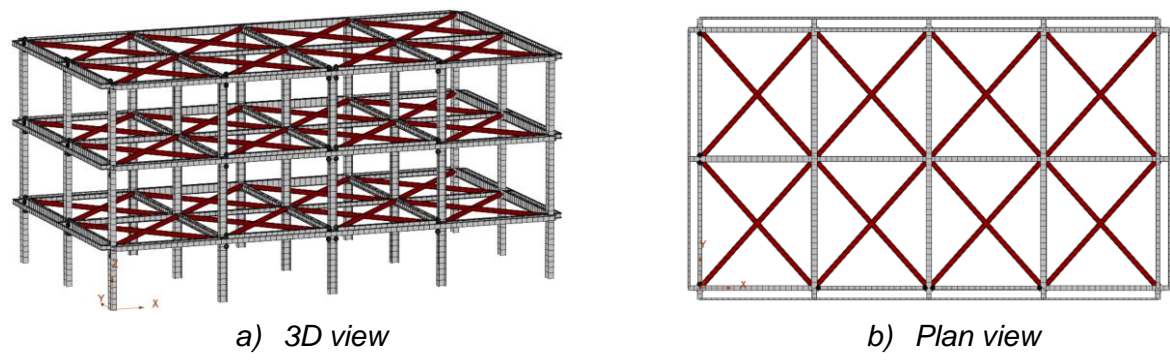


Figure 3. Slab diaphragm effect modelling

The loads perpendicularly applied on the one-way slabs were assigned to the supporting beams as uniform line loads estimated based on the direction of slab load transfer and tributary areas. The accidental load combination was considered in the analyses according to the prescriptions of (EN 1990, 2002).

$$\sum_{j\geq 1} G_{k,j} + A_d + \psi_{1,1} Q_{k,1} + \psi_{2,i} Q_{k,i}$$
 eq. 1

The permanent and variable actions ($G_{k,j}$ and $Q_{k,1}$) were taken identical to the ones used in the regular design of the building for the Serviceability Limit State (SLS) and Ultimate Limit State (ULS) as reported in Table 1. No specific values for the accidental action A_d were considered in the structural model as this action represents the loss of a supporting column (i.e. A_d is in this case the removal of a support). A combination factor $\psi_{1,1}$ =0.5 as recommended in the Eurocodes was used for the variable loads $Q_{k,1}$, even though the Italian normative (NTC, 2018) allows using a less demanding combination factor $\psi_{1,1}$ =0.3 for office buildings in accidental situations.

Table 1. Design loads

Load	Type	1 st floor	2 nd floor	3 rd floor
Dead load (kN/m²)	$G_{k,1}$	5.35	5.35	4.15
Live load (kN/m²)	$Q_{k,1}$	3.0	3.0	-
Cladding (kN/m)	Q k,1	4.4	4.4	-
Snow load (kN/m²)	$Q_{k,2}$	-	-	0.6

3.2. Modelling of FREEDAM joints

The structural robustness of a building strongly depends on the local behaviour of structural members and their end connections. Depending on their characteristics (e.g., stiffness, strength, and ductility), the joints may significantly influence the distribution of internal forces and displacements in frame structures as well as the ultimate structural capacity and residual strength.

Typically, the behaviour of joints is integrated in structural analyses through rotational springs simulating the response of joints under bending action. However, this modelling approach does not allow for a proper consideration of the moment-axial force (*M-N*) interaction in the joints, which makes it unsuitable for simulations of column losses where the joints may be subject to such combinations of internal forces once catenary actions develop in the part of the structure that bridges over the lost column.

3.2.1. Simplified two-spring model

Based on the well-known component method introduced in EN 1993-1-8 (2005), a simplified two-spring model (2SM) for FREEDAM joints was developed and validated against experimental evidence by D'Antimo (2020) and Santos et al. (2020). The model consists of two extensional springs (top and bottom) interconnected by rigid elements as represented in Figure 8a. An additional rigid shear spring ensures the transfer of shear forces at the beam ends. The so-built model accommodates the *M-N* interaction and accounts for the behaviour of basic joint components characterised by extensional springs with nonlinear behaviour laws (see Figure 4b-c) derived with the component method of EN 1993-1-8 (2005). As demonstrated by Santos et al. (2020), the component method can be effectively extended to characterise both pre- and post-sliding behaviour of the FREEDAM joints. The plastic range of behaviour for basic joint components is characterised

by a strain-hardening stiffness and an ultimate strength analytically estimated as proposed by Jaspart et al. (2019).

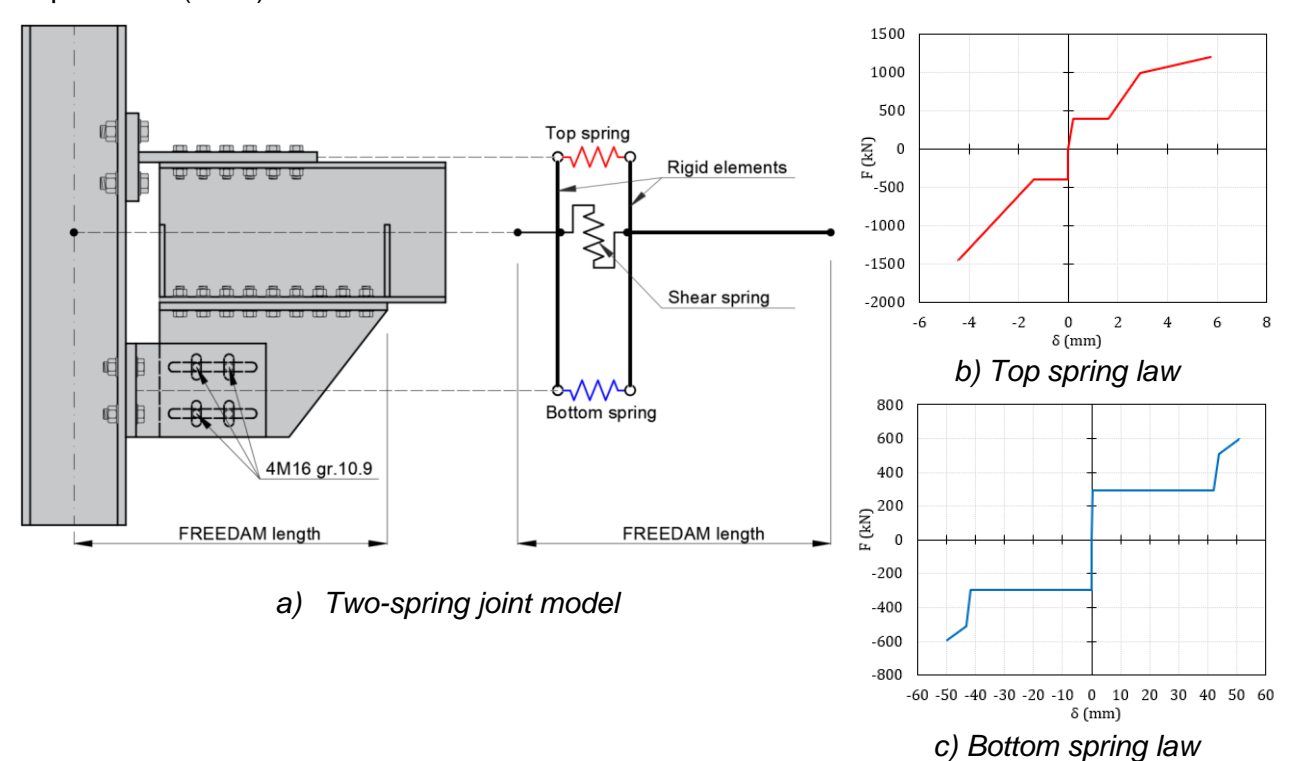


Figure 4. FREEDAM joint modelling

3.2.2. Model validation

The reliability of the simplified 2SM was validated through comparisons with results of experimental tests performed on real scale joints extracted from the DREAMERS building as reported in the project deliverable D4.2 and reflected in Figure 5. In addition to previous validation against experimental and numerical results, the two experimental tests performed at the University of Liege allow validating the 2SM in terms of both pre- and post-sliding behaviour of FREEDAM joints with account for full-range response up to joint's failure as reflected in the next sections.

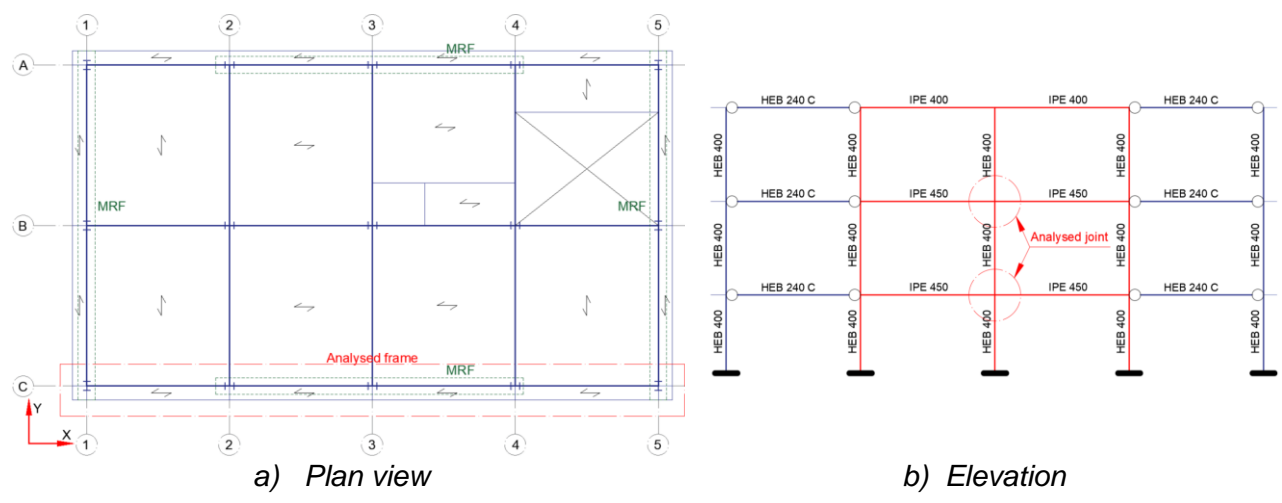


Figure 5. Extraction location of the analysed joint

3.2.2.1. Validation for full-range response under bending moment

The first experimental test presented in deliverable D4.2 was performed to characterise the full-range behaviour of FREEDAM joints under bending moment. To validate the spring model, the test was numerically simulated using the 2SM with the spring behaviour laws given in Figure 4b-c combined with classical beam elements in the FINELG FE software. The numerical model overlapped with the configuration of the test specimen is schematically represented in Figure 6.

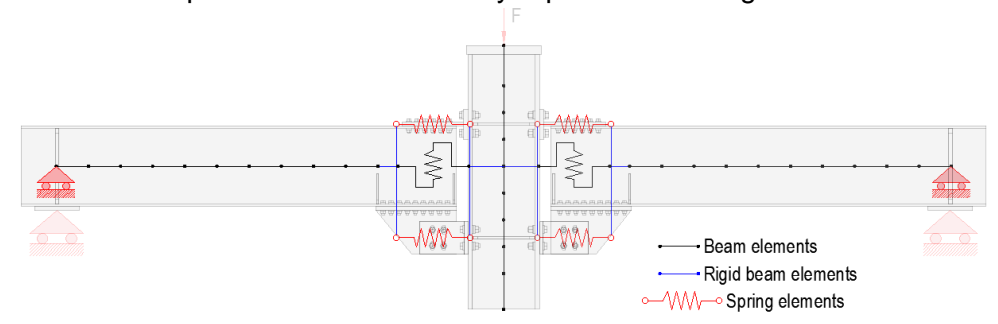


Figure 6. Schematic view of the numerical model – Test 1

The prediction in terms of applied force vs. vertical displacement recorded during testing at the level of the column is given in Figure 7a. The results reveal some inconsistencies between the experimental force-displacement curve and the prediction of the 2SM in terms of overall curve shape and the ultimate capacity of the specimen. These inconsistencies arise from the approach used to characterise the behaviour of the friction damper integrated in the 2SM. The initial modelling approach used to simulate the response of the damper doesn't account for any preload loss that occurs in the preloaded high-strength (HS) M16 damper bolts along the slippage phase (2SM-w/oPL). This leads to an overestimation of the ultimate capacity of the specimen (6.4% overestimation) as well as to an overall plateau-shaped *F-d* curve along the slippage phase of the dampers.

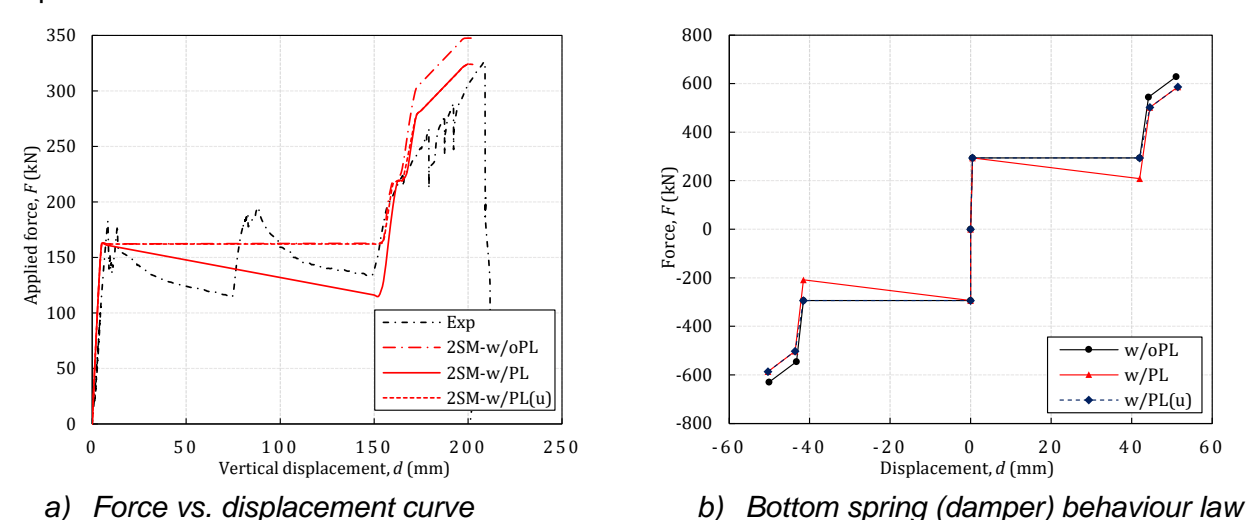


Figure 7. Simplified 2SM validation – Test 1

Nonetheless, experimental observations and measurements taken during the second test presented in deliverable D4.2 allowed concluding that an averaged 29% preload loss was registered during the slippage phase of the damper. This conclusion has been endorsed by the experimental measurements taken during the tests performed at the University of Salerno where similar decrease of the preload force in the damper bolts were recorded (see deliverable D4.1).

To account for the expected preload loss, the behaviour law assigned to the lower spring of the 2SM was modified by integrating the 29% preload loss (PL) as a linear decrease along the slippage phase of the damper (w/PL behaviour law in Figure 7b). However, since the resistance decay along the slippage phase due to the preload loss is not an indicative of the joint's robustness but rather a phenomenon that influences mainly the hysteretic energy dissipated under seismic excitation, an additional way of characterising the behaviour of the components acting at the level of the damper was considered for robustness-related investigations. This behaviour law disregards the resistance decay along the slippage phase of the damper, yet it accounts for the effects of preload loss on the ultimate resistance of the damper assembly (see behaviour law w/PL(u) in Figure 7b). This modelling approach safely idealises the joint behaviour in the slippage phase through a plateau, which in turn allows performing stable numerical simulations in robustness-related scenarios accounting for the actual post-slippage behaviour of the joints.

Therefore, three numerical models were built by implementing the preload loss in the HS M16 bolts of the friction dampers in three different ways as follows:

- 2SM-w/oPL: the 2SM without any preload loss considered
- 2SM-w/PL: the 2SM with the preload loss considered linear along the slippage phase of the dampers and integrated in the ultimate capacity of the joint
- 2SM-w/PL: the 2SM with the preload loss integrated only for the ultimate capacity of the joint with a plateau-shaped slippage phase of the dampers.

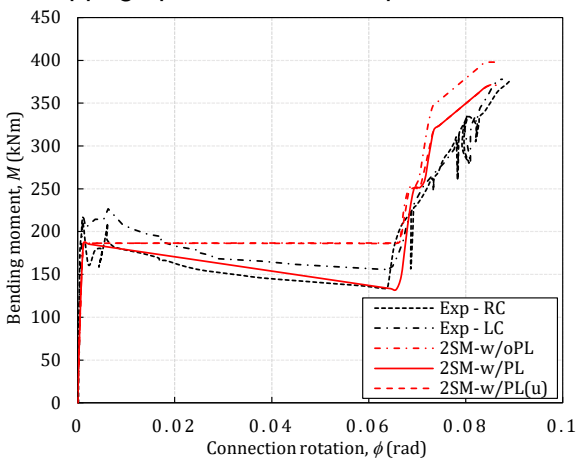


Figure 8. Predicted moment vs. rotation curves – Test 1

Figure 8 reflects the comparison between the predicted and the experimental moment-rotation curves for the right and left connections (RC and LC) of the tested joint. Generally, the 2SM shows a good performance for predicting the full-range behaviour of the FREEDAM joints, although the results reveal the model sensitivity to the characterisation of basic joint components. Indeed, the behaviour law considered for the characterisation of the friction damper plays a crucial role in achieving accurate predictions in terms of both deformation and strength capacities.

It is evident that in order to accurately predict the ultimate capacity of the connections, the preload loss in the HS M16 bolts and its inherent effects on the friction resistance of the dampers should be considered. For both cases where the expected preload loss was considered (2SM-w/PL and 2SM-w/PL(u)), the 2SM provides predictions with acceptable accuracy for the full-range behaviour of the tested joint with a notable perfect match between the recorded and predicted ultimate moment resistance and deformation capacities, both parameters being of key importance for assessing the robustness of the joints.

3.2.2.2. Validation for full-range response under a virtual column loss

The performance of the 2SM is analysed hereinafter in the context of FREEDAM joints subjected simultaneously to bending moment and axial forces, a situation that corresponds to the load combination typically acting on joints in column loss scenarios. The experimental results of Test 2 performed at the University of Liege and reported in deliverable D4.2 are used to assess the capability of the 2SM to replicate the full-range behaviour of FREEDAM joints subjected to quasistatic column removals.

Similar to the model validation under applied monotonic bending, the test specimen was numerically modelled in the FINELG FE software. The schematical view of the numerical model comprised of the 2SM combined with classical beam elements is represented in Figure 9 overlapped with the 2D view of the test specimen.

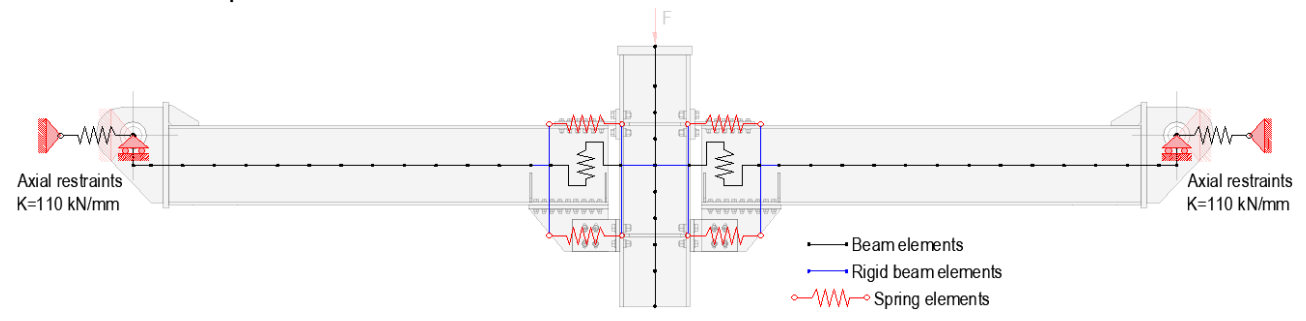


Figure 9. Schematic view of the numerical model – Test 2

The axial restraints provided in the numerical model through extensional springs simulate the deformability of the experimental in-plane restraining system. The axial stiffness of these restraints was estimated based on experimental recordings of the axial forces in the beams of the specimen and the corresponding horizontal displacement recorded at the extremities of the test specimen. As reflected in Figure 10, the axial stiffness of the in-plane restraining system was estimated at 110 kN/mm, and this stiffness was assigned to the extensional springs at the extremities of the numerical model to account for the actual boundary conditions provided by the test rig.

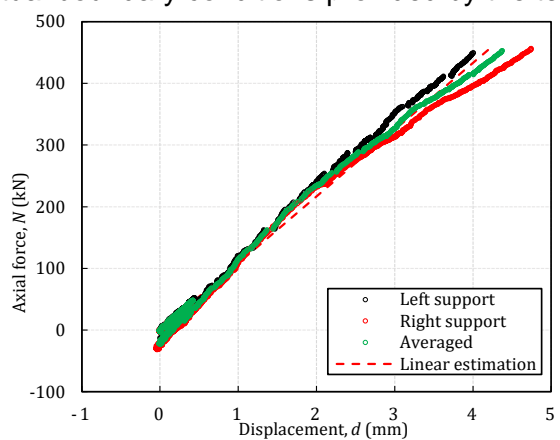


Figure 10. Beam axial force vs. lateral support horizontal displacement

The behaviour laws assigned to the springs of the 2SM were taken identical to the ones used for validating the model against the experimental results of Test 1 as reported in the previous section. The comparison between the predicted and experimental force-displacement curves shown in Figure 11 reveal once again the sensitivity of the 2SM to the method used for characterising the behaviour of basic joint components. In particular, the implementation of the effects of preload losses in the response of the friction damper seems to govern the accuracy of predictions provided by the 2SM.

It is worth noting that the best agreement between the prediction and experimentally observed response is provided by the numerical model in which the preload loss was considered as occurring along the slippage phase of the dampers with inherent effects over the friction and ultimate resistance of the FREEDAM joints (2SM-w/PL).

However, an acceptable prediction is also provided by the numerical model in which the preload loss was considered as affecting exclusively the ultimate strength of the joint (2SM-w/PL(u)) and the slippage phase characterised by a plateau. Although the decay in the applied force along the slippage phase of the connections is not captured, the model provides an identical post-slippage response in terms of stiffness and ultimate capacity as the 2SM-w/PL model.

An overestimation of the specimen's ultimate capacity of approximately 9% is observed for both numerical models in which the preload loss was implemented. This discrepancy may be attributed to the fact that the experimental test was stopped due to safety reasons before reaching the actual ultimate capacity of the specimen which would correspond to the brittle rupture of the damper bolts subjected to shear. Indeed, since the actual failure was not reached, some residual strength should be envisaged. This was highlighted by the perfect agreement between the predicted and actual capacity of the specimen used in Test 1 where the ultimate failure was reached during the test.

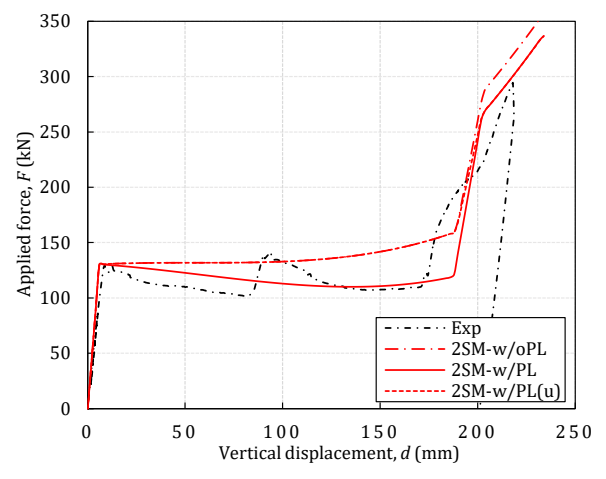


Figure 11. Applied force vs. vertical displacement curves

Figure 12 shows the development of catenary action in the beams of the specimen during testing and the predictions provided by the three numerical models. It is worth noting that the evolution of beam axial forces seems to be insensitive to the approach chosen to characterise the response of the friction damper with respect to the bolt preload loss.

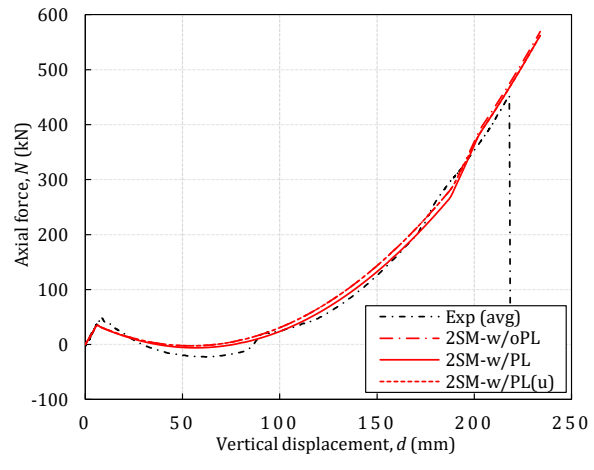


Figure 12. Beam axial force vs. vertical displacement curves

As mentioned in the previous section, in contrast to the beam axial force, the evolution of the bending moment at the level of connections is highly reliant on the considered response of the friction damper. This observation is endorsed by the results reported in Figure 13 where the comparison between the experimental response of the right connection (RC) and the numerical prediction highlights the accuracy of the 2SM in replicating the behaviour of the FREEDAM joint under combined M-N when the preload loss is accounted for.

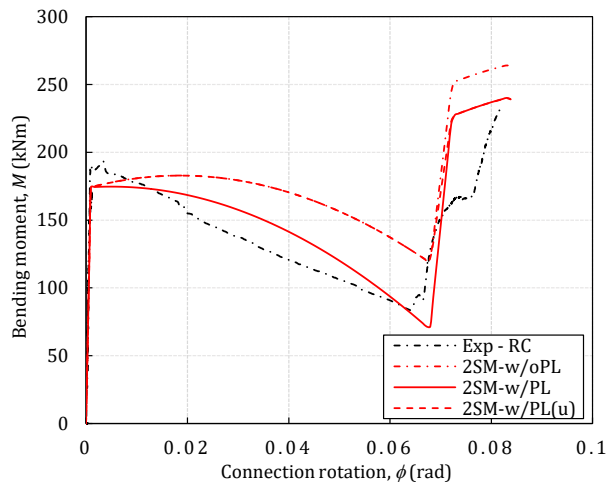


Figure 13. Connection moment vs. rotation curves

The results discussed in the previous sections prove the suitability of the 2SM for numerical studies in which the full-range behaviour of FREEDAM joints is of interest. Moreover, for robustness-related investigations such as simulations of column loss scenarios in which the proper integration of the post-slippage response of the FREEDAM joints is critical, the validation of the 2SM allowed identifying an acceptable compromise in terms of model complexity.

The identified modelling solution accounts for an expectable preload loss of 29% at the damper stroke limit which affects the ultimate capacity of the overall FREEDAM joint (w/PL). However, in order to ensure the convergence of large numerical simulations performed on global structural models, the preload loss can be considered as affecting exclusively the ultimate capacity of the joints (w/PL(u)). Therefore, the slippage phase of the damper's response can be defined as a plateau, and the effects of the preload loss can be integrated into the estimation of the damper's ultimate resistance as reflected in Figure 14. This modelling approach eliminates the need for introducing response regions with negative stiffness, which in turn facilitates the convergence for numerical solvers with a marginal influence on the overall accuracy of the results when the post-slippage response of FREEDAM joints is of concern. In the following sections, this approach is used for numerical simulations for column loss scenarios proposed for the evaluation of robustness of the DREAMERS pilot building.

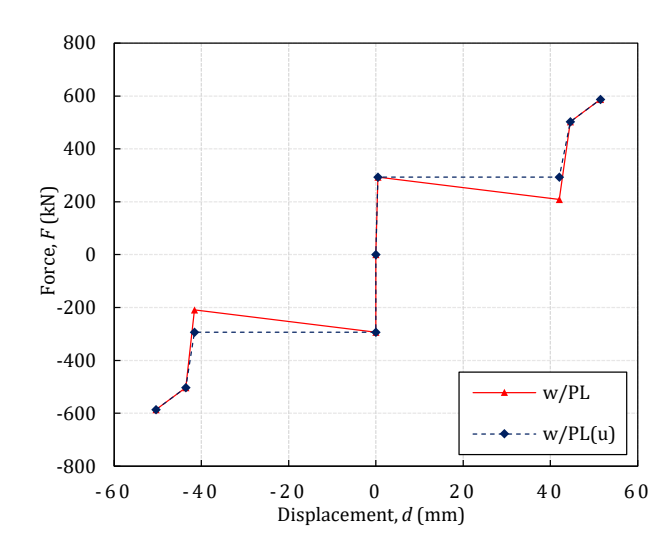


Figure 14. Behaviour laws for the assembly of components active at the damper level

4. Structural robustness under column loss scenarios

The loss of supporting columns in the pilot building was simulated through a two-sequence analysis. For the first sequence, the lost column was replaced by a reaction force equal to the column design axial force N_d in the accidental load combination. The second sequence initiates a nonlinear analysis in which an incremental downward force $F=\lambda N_d$ was applied at the same location as N_d as depicted in Figure 15.

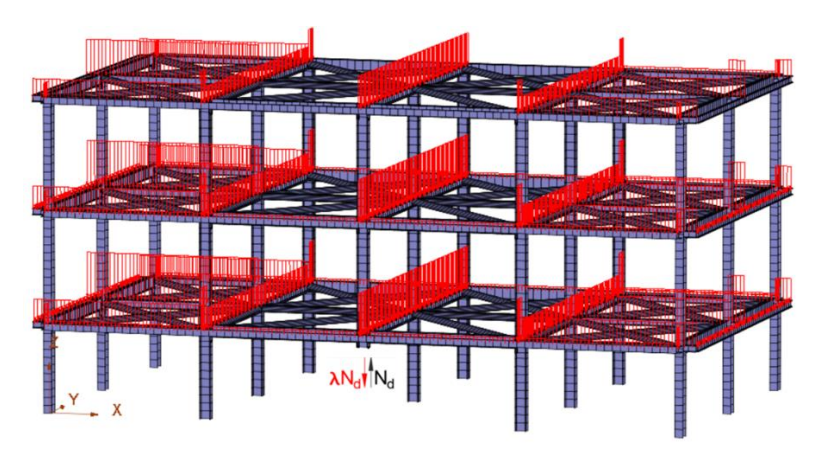


Figure 15. Column loss loading sequence

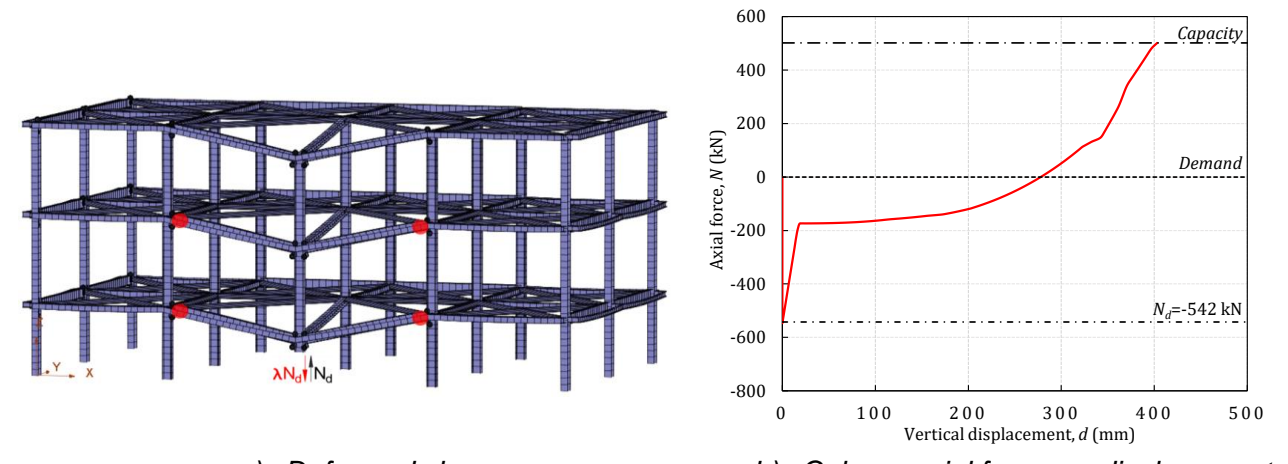
The evolution of the axial force N in the lost column is then plotted with respect to the vertical displacement d of the force application point. The full nonlinear structural response is thus characterised by a force-displacement N-d curve (pushdown curve) which is used further to evaluate the robustness of the structure under the considered column removal scenario.

4.1. Structural robustness under perimeter column loss scenario

4.1.1. Robustness of the bare steel structure (BSS)

To evaluate the response further to the assumed column removal, the pilot building was initially considered as a bare steel structure (BSS). This allows drawing conclusions on the robustness of the main structural system as well as observing the local contribution of the FREEDAM joints for

collapse resistance. Figure 16 depicts the structural behaviour of the pilot building under the perimeter column loss (Scenario 1).

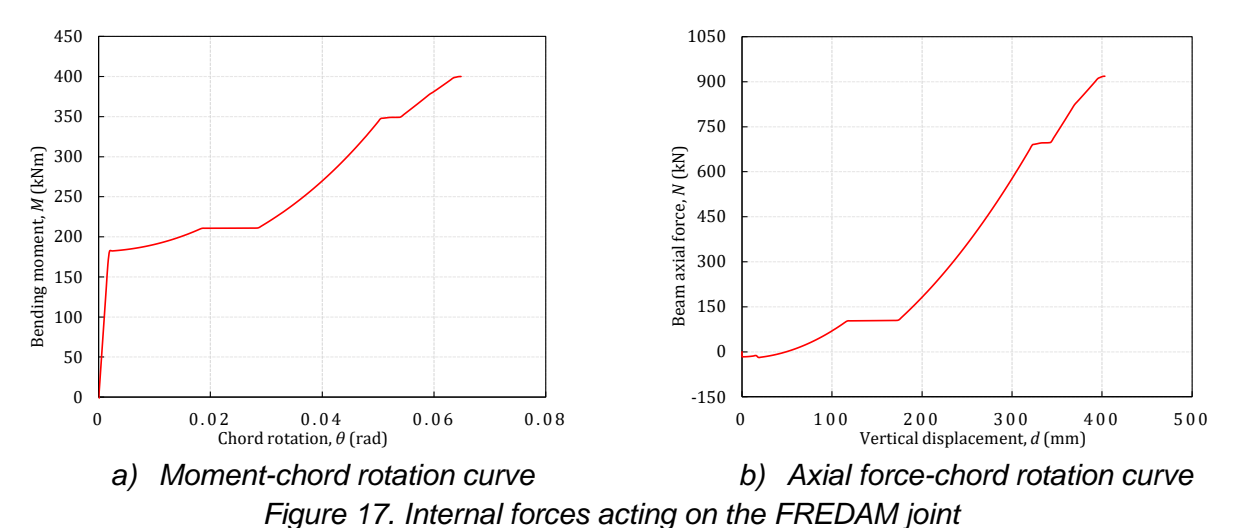


a) Deformed shape b) Column axial force vs. displacement Figure 16. BSS response under the perimeter column loss (Scenario 1)

It is noticeable that the large rotational capacity of the dissipative joints provided in the two bays adjacent to the lost column allows for the development of significant membrane forces in the beams (920 kN) of the directly affected part (DAP). This enables the structure to sustain the column loss with significant residual strength yielding a Demand/Capacity (D/C) ratio D/C=0.52.

The collapse is triggered by the successive failure of the FREEDAM joints located at the 1st and 2nd storeys (highlighted in red in Figure 16a) which are subjected to a combination of hogging moment and axial tensile force that leads to the failure of the T-stub in bending component (upper spring in the 2SM).

Figure 17 shows the variation of internal forces with respect to the chord rotation in the failing joints. The evolution of internal forces within the structure reveals some important peculiarities related to the behaviour of the FREEDAM joints and the fact that the structural response of buildings equipped with such joints is quite different when compared to structures with conventional joints subjected to column losses.



More specifically, as shown in Figure 18, the bending moment acting on the joints at the extremities of the DAP increases even after membrane forces start emerging in the beams connected to the lost column. This can be seen as in opposition to what is normally observed in structures with

conventional semi-rigid joints as proved by Demonceau (2008), Marginean (2017), and Kozlowski & Kukla (2019) among others.

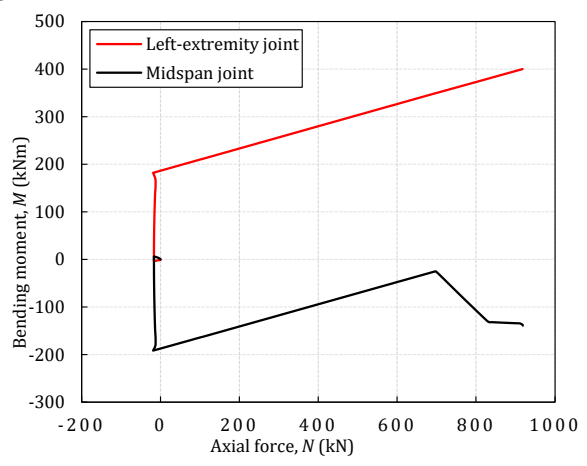


Figure 18. M-N evolution in the 1st floor joints of the DAP

This difference comes from the influence of the friction damper response on the distribution of internal forces within the joint. Indeed, the evolution of forces in the two springs of the 2SM depicted in Figure 19 may clarify this issue. Once the damper has reached its friction resistance, the overall joint has reached its sliding moment capacity and rotates with almost no further moment increase. As soon as the vertical displacements become significant (approx. 170 mm and 0.03 rad chord rotation), the beams are engaged in catenary action and significant axial tension develops. This tension is eccentrically transferred from the beam cross-section to the joint cross-section, thus inducing a bending moment. Furthermore, since the damper (lower spring) enters in the slippage phase, its resistance remains constant (friction resistance). To ensure the compatibility of displacements and the equilibrium on the joint cross section, the upper spring (T-stub) is overloaded in tension, which leads to the increase of the bending moment appearing at the joint level and to the subsequent failure of the T-stub.

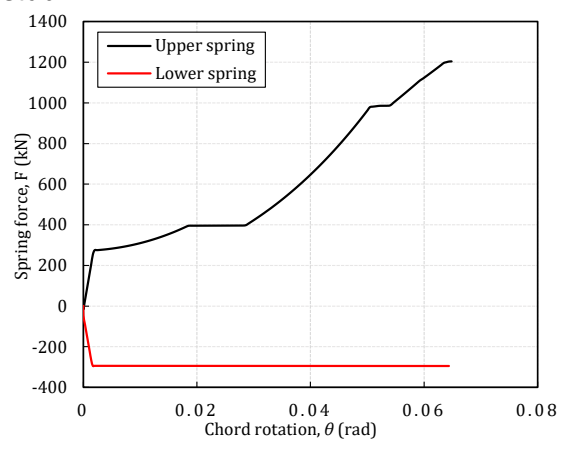


Figure 19. Evolution of forces in the 2SM for joints at the extremities of the DAP

4.1.2. Robustness contribution of non-structural façade elements

In addition to the collapse resistance of the bare steel structure (BSS) investigated in the previous section, complementary resisting mechanisms ensured by the interaction between structural elements and non-structural infill façade walls can be envisaged.

An experimental campaign performed by Landolfo et al. (2019) on exterior façade walls subjected to seismic action revealed that, depending on their connectivity to the surrounding structural members,

these non-structural elements exhibit a non-negligible stiffness and strength when resisting in-plane loads. The main outcomes of the experimental programme were reported in terms of fragility curves for façade (and partition) walls that correlate the extent of damage observed on non-structural walls to the Inter-storey Drift Ratios (IDRs) as illustrated in Figure 20.

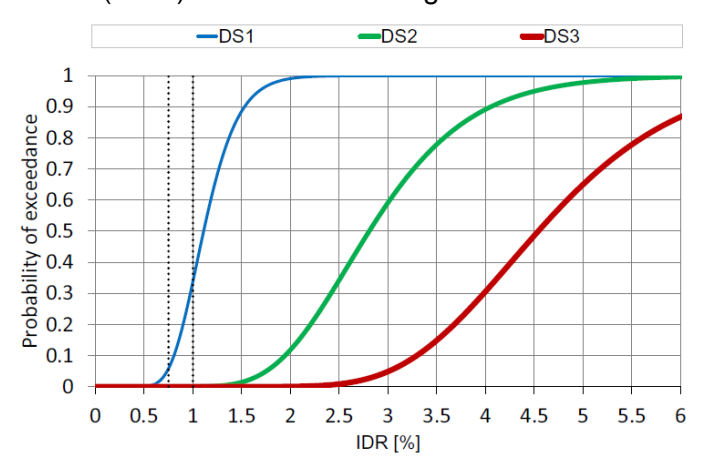


Figure 20. Fragility curves for façade walls with enhanced connections subjected to dynamic loads (Landolfo et al. (2019))

For façade walls with enhanced anti-earthquake connections such as the ones used on the perimeter of the DREAMERS building, the results of seven experimental tests performed under cyclic loads (ground motion) with different intensities allowed deriving a simplified backbone curve that characterises the individual response of façade walls subjected to in-plane loads. In Figure 21, the red thick curve represents the so-determined backbone curves based on the peak resistance of each specimen reached throughout testing. This can be viewed as a behaviour law of façade panels subjected to in-plane horizontal loads.

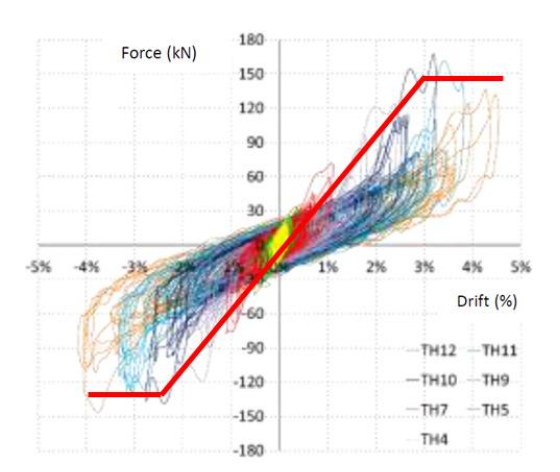


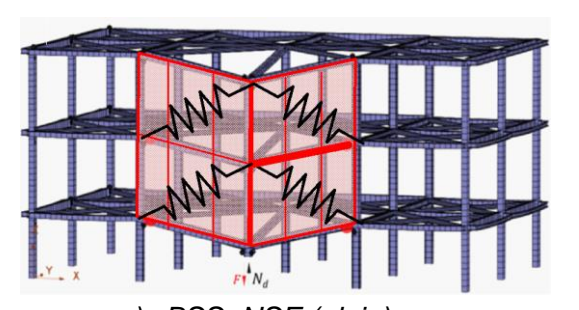
Figure 21. Fragility curves for façade walls with enhanced connections subjected to dynamic loads (Landolfo et al. (2019))

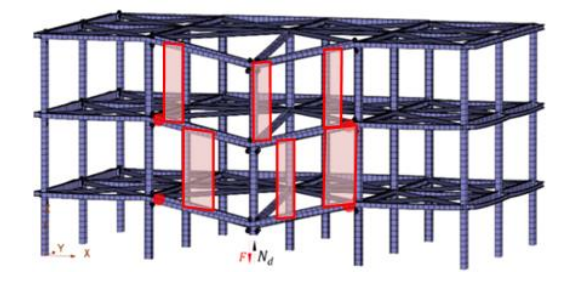
Due to the lack of experimental evidence on the response of façade panels subjected to vertical (along the panel) in-plane loads, a series of simplifying assumptions had to be made in order to integrate the behaviour of non-structural façade panels in column loss simulations:

- The response of panels is assumed to be identical for both horizontal and vertical in-plane loads

- For column loss scenarios, the concept of IDR can be assimilated with an equivalent relative drift between the ends of a bay (span) adjacent to the lost column
- The ultimate failure of the façade panels occurs for an IDR=4.5%.

Based on these assumptions, the façade walls were integrated into the FE model by adding several shear springs as depicted in Figure 22a. The behaviour laws assigned to these springs were derived based on the generic backbone curve defined in Figure 21 with account for the dimensions of the façade panels used in the DREAMERS building.





a) BSS+NSE (plain)

b) BSS+NSE (actual)

Figure 22. Schematical view of façade panels integration in the FE model

Initially, the panels were considered to cover the entire surface of the façade in the spans adjacent to the lost column (BSS+NSE (plain) in Figure 22a). However, given the big glassing surface of the façade, the actual dimensions of the façade panels can diminish the contribution of these elements. To cover this issue, an additional model has been built to account for the actual configuration of the façade where the façade surface covered by windows and glassing was considered as non-collaborative to the resisting system (BSS+NSE (plain) in Figure 22b).

Non-linear FE analyses were performed on the so-built models to assess the influence of non-structural façade panels on the overall structural robustness of the pilot building in case of a perimeter column loss (Scenario 1). The results reported in Figure 23 show that the contribution of these elements is far from being negligible. Moreover, if façade panels are assumed on the entire surface of the façade (BSS+NSE (plain)), the structure exhibits an enhanced response characterised by higher stiffness during the slippage phase of the FREEDAM connections and significantly higher ultimate capacity with a D/C ratio of 0.48, which denotes a better behaviour even when compared to the BSS response (D/C=0.52), despite the slightly lower deformation capacity (ductility).

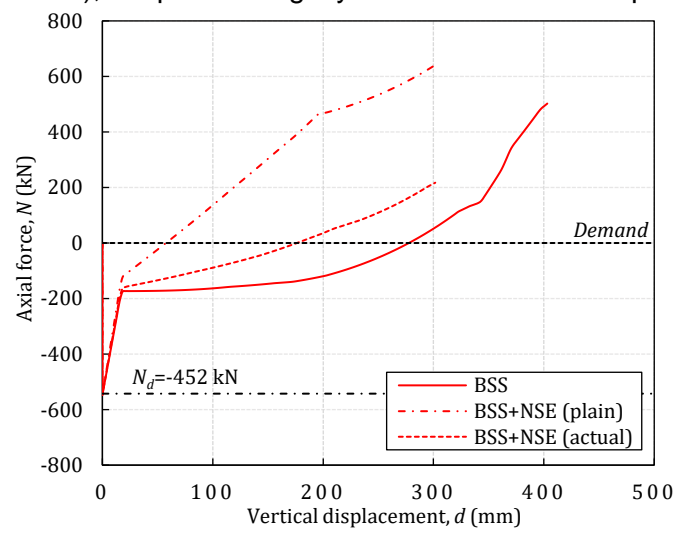


Figure 23. Column axial force vs. displacement further to the perimeter column loss

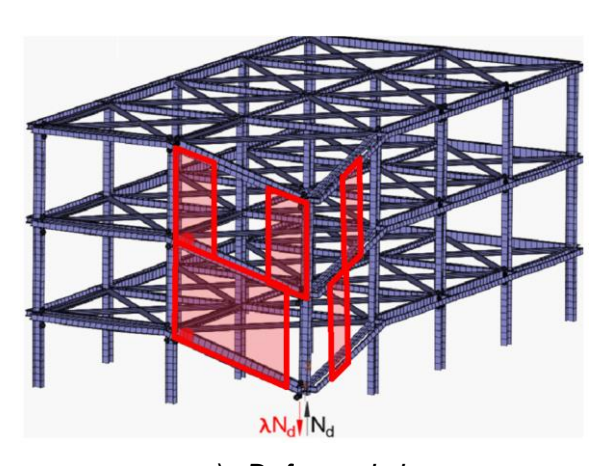
The integration of panel dimensions in the numerical model (BSS+NSE (actual)) show that, in the actual configuration, the façade panels have a contribution to the structural robustness, albeit limited when compared to the ideal case of plain panels. The limited ductility supply is governed by the failure of façade panels assumed to occur at an IDR of 4.5% and a 50% probability of exceedance of DS3 as per the fragility curves given in Figure 20. Considering the actual configuration of the façade, the actual D/C ratio corresponding to this failure criterion is approximately 0.67. Therefore, it is reasonable to assume that the pilot building survives the investigated perimeter column removal with a 33% resistance reserve. It is worth noting that this D/C ratio corresponds to the failure of the non-structural façade panels. In reality, after the failure of these panels, the structural response is expected to reflect the BSS case (where the façade panels were neglected), thus leading to the same D/C ratio found for the BSS case (i.e., D/C=0.52).

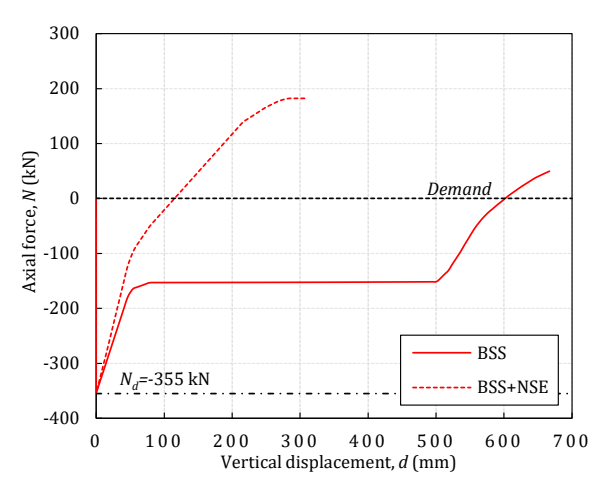
4.2. Structural robustness under corner column loss scenario

The loss of a corner column tends to be one of the most demanding scenarios in terms of robustness. In this case, due to the lack of axial restraints at one end of the orthogonal beams intersecting at this location, the development of catenary actions is prevented. The main resisting scheme in this case is represented by the plastic mechanism of the beams which, in the pilot building, is governed by the ultimate resistance of the FREEDAM joints.

It is worth noting that on the Y direction perimeter MRFs, the joints on the first 2 floors are equipped with a D2 FREEDAM device, and exhibit a higher ultimate bending capacity of $M_{u(D2)}$ =520 kNm in comparison to the joints on X direction (D1 devices) with an ultimate bending capacity of $M_{u(D1)}$ =365 kNm.

Since in this case the catenary action cannot be mobilised due to the lack of axial restraints, the joints are mainly subjected to bending. Thus, exclusively due to the considerably enhanced bending resistance of the FREEDAM joints on Y direction, the structure sustains the assumed corner column loss with a D/C ratio of 0.87 when the bare steel structure is considered (BSS in Figure 24b). The collapse is triggered by the premature failure in shear of the bolts at the level of the friction devices.





a) Deformed shape

b) Column axial force vs. displacement

Figure 24. Structural response under the corner column loss (Scenario 2)

The response of the BSS is enhanced by the contribution of the façade panels that are present in the DAP as illustrated in Figure 24. The non-linear FE analysis performed on the numerical model that incorporates the façade non-structural elements (BSS+NSE) reveal that the structural robustness is tremendously improved due to the mobilisation of higher stiffness provided by the façade panels along the slippage phase of the dissipative joints. The C/D ratio increases up to 0.66,

thus proving the ability of the pilot building to survive the loss of the corner column with much lower ductility request at the level of the joints.

4.3. Structural robustness under internal column loss scenario

The pushdown curve reported in Figure 25b (where $F=\lambda N_d$) reveals that, to survive an internal column loss, the beams and their simple end-connections should provide sufficient rotation capacity and resistance to accommodate a vertical displacement of 232 mm. If these two criteria are fulfilled, the tensile forces in the directly affected part (DAP) of the structure bridging above the lost column reach values of 1810 kN and 1940 KN for the beams on X and Y direction respectively (see Figure 26).

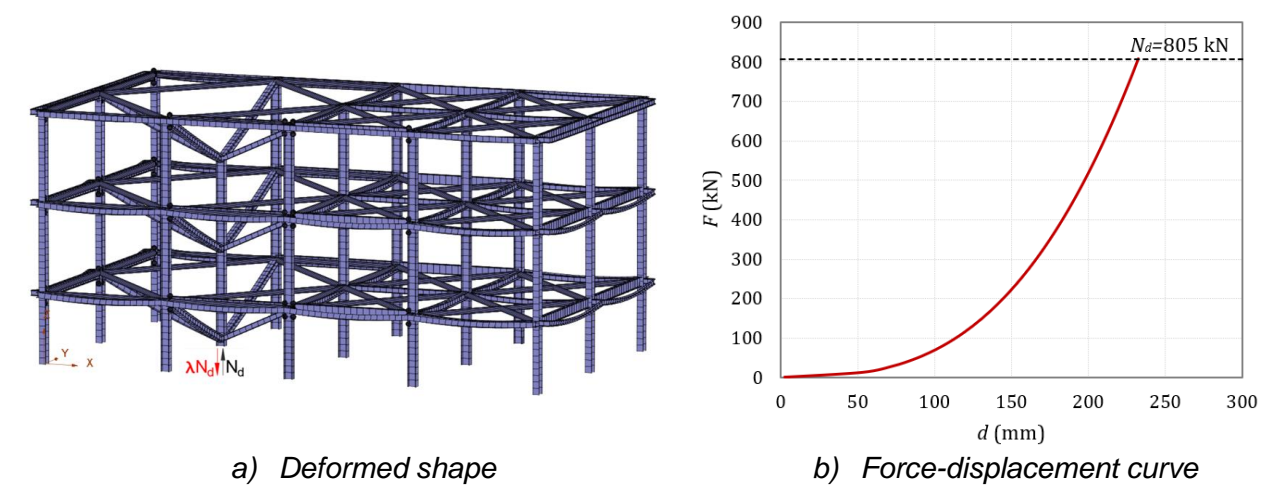


Figure 25. Structural response under the internal column loss (Scenario 3)

This distribution of tensile forces is valid for the beams of all storeys and, if compared to the tensile resistance required by the tying method of EN 1991-1-7 (2006), they are approximately tenfold greater than the normative demand (1940 kN against 205.7 kN obtained with the tying method). As demonstrated previously within the normative design for robustness reported in deliverable D2.2, the simple end-connections of the internal beams exhibit an ultimate tensile resistance of maximum 429.1 kN. This proves to be considerably lower than the actual demand associated with the column loss scenario.

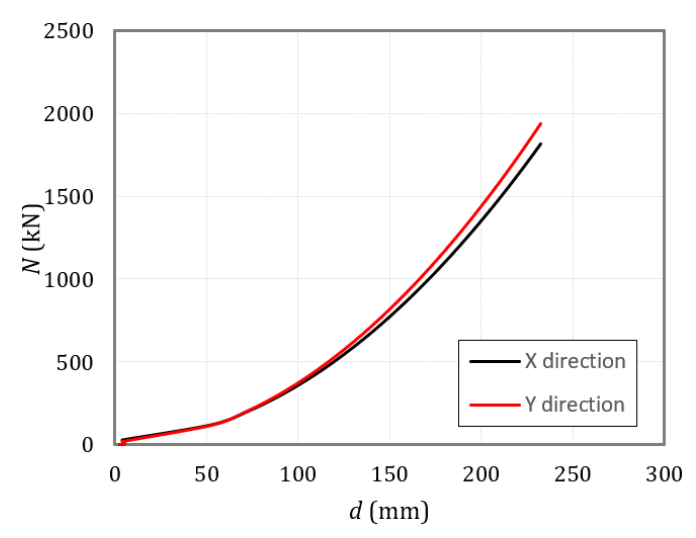


Figure 26. Evolution of tensile forces in the beams of the DAP

Normally, solutions to enhance the resistance of the simple connections could be envisaged; however, such measures would lead to unrealistic/unpractical solutions for the simple (hinged) joints as highlighted in the FAILNOMORE Design Manual (Demonceau et al., 2021). Therefore, to resist these high tensile forces, semi-rigid joints should be used instead of simple connections; yet this change is to be avoided for the pilot building due to its influence on the structural seismic performance thus implying a redesign of the structure.

The alternative is to prevent the column loss that triggers the collapse by designing the column as a *key element*. Practically, as prescribed in EN 1991-1-7 (2006), the normative method is to design the column so that it is capable of sustaining an accidental design action of 34 kN/m² applied in horizontal and vertical directions (one at a time) to the column and any components attached to it.

This method is applied to the internal column and, at first, the horizontal application of the recommended accidental action is analysed. To cover the worst-case scenario, the uniformly distributed load of 34 kN/m² is applied on the column's cross-section height (weak axis) as a line load. Note that it is assumed that there are no other (non-structural) components attached to the column on this direction. Given the relatively small surface on which it is distributed, this load induces trivial bending moment and shear force in the column (M_{Ed} =17 kNm and V_{Ed} =26.2 kN) as shown in Figure 27.

As demonstrated in deliverable D2.2, the column base connections remain in the elastic range for internal forces significantly higher than the ones reported in Figure 27. This allows concluding that the element sustains the horizontal accidental load recommended for key members.

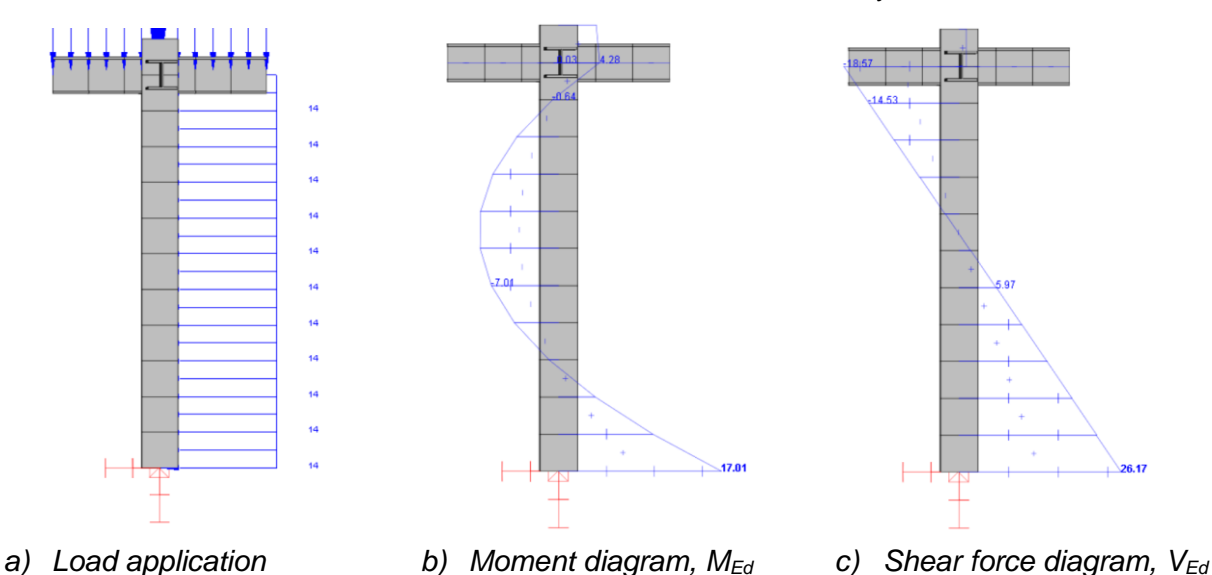


Figure 27. Structural response under the internal column loss

5. Conclusions

The robustness assessment presented in this document serves as a complementary research-oriented study on the robustness of the pilot building through advanced FE analyses. The structural performance of the pilot building was analysed for three column loss scenarios. For this purpose, a simplified two-spring model (2SM) was validated against experimental evidence. The comparisons between the predictions provided by the 2SM and the experimental results proved the adequate accuracy of the model and endorse its use for the modelling of FREEDAM joints in nonlinear pushdown analyses simulating static column removals.

The outcomes of the conducted investigations allow drawing the conclusions that the pilot building is robust enough to sustain a perimeter or a corner column loss occurring in the MRFs equipped with FREEDAM joints.

In addition to the integration of the full-range behaviour of the dissipative joints, non-linear numerical analyses were performed on 3D models with account for the potential contribution of non-structural façade panels. Experimental evidence gathered in previous studies allowed defining a simplified behaviour law for this type of elements. The latter was subsequentially incorporated in numerical models to simulate the façade panels through equivalent shear springs and allowed concluding on the beneficial effects of infill façade panels on the overall structural robustness.

Some concerning observations were made with respect to the insufficient structural robustness of the building in case of internal column losses. This is mainly due to the fact that the simple joints provided in the inner bays of the building are not capable of withstanding the high membrane forces developing in the beams of the DAP. This confirms the findings of previous research works (e.g., FAILNOMORE) and, at the same time, questions the reliability of the tying method of EN 1991-1-7. In fact, as stated in FAILNOMORE design manual, the tying method as proposed in EN 1991-1-7 has to be seen as a method which allows providing a minimum level of continuity between structural elements, and which is a necessary but insufficient measure for ensuring the survival of a building structure in case of full column removal.

The only viable solution for the pilot building is to prevent the loss of the internal column, thus making it a key element. However, the standard requirements for key elements lead to very low demands in terms of strength and stability, and it was proven that, upon the application of the accidental load recommended for key elements, the column fulfils the normative demand.

REFERENCES

- D'Antimo, Marina. 2020. "Impact Characterization of Innovative Seismically Designed Connections for Robustness Application." Université de Liège, Liège, Belgique. https://orbi.uliege.be/handle/2268/246289.
- Demonceau, J. F., Tudor Golea, J. P. Jaspart, Ahmed Elghazouli, Zeyad Khalil, Aldina Santiago, Ana Francisca Santos, et al. 2021. *Design Recommendations against Progressive Collapse in Steel and Steel-Concrete Buildings*. ECCS-European Convention for Constructional Steelwork. https://www.steelconstruct.com/eu-projects/failnomore/design-manuals/.
- Demonceau, Jean-François. 2008. "Steel and composite building frames: sway response under conventional loading and development of membrane effects in beams further to an exceptional action." PhD Thesis, Université de Liège.
- EN 1990. 2002. Eurocode Basis of Structural Design. Brussels: European Committee for Standardisation.
- EN 1991-1-7. 2006. Eurocode 1 Actions on Structures Part 1-7: General Actions Accidental Actions. Brussels: European Committee for Standardisation.
- EN 1993-1-8. 2005. Eurocode 3 Design of Steel Structures Part 1-8: Design of Joints. Brussels: European Committee for Standardisation.
- Jaspart, Jean-Pierre, Adrien Corman, and Jean-François Demonceau. 2019. "Ductility Assessment of Structural Steel and Composite Joints," September. https://orbi.uliege.be/handle/2268/239363.
- Kozlowski, Aleksander, and Damian Kukla. 2019. "Experimental Tests of Steel Unstiffened Double Side Joints with Flush and Extended End Plate." *Archives of Civil Engineering* 65 (4): 127–54. https://doi.org/10.2478/ace-2019-0051.
- Marginean, Ioan. 2017. "Robustness of Moment Steel Frames under Column Loss Scenarios." Politehnica University of Timisoara.
- NTC. 2018. "Norme techniche per le construzioni." Ministero delle Infrastrutture e dei Trasporti.
- prEN 1993-1-14. 2021. "Design of Steel Structures Part 1-14: Design Assisted by Finite Element Analysis." European Committee for Standardisation, Brussels.
- Landolfo, Raffaele, Tatiana Pali, Bianca Bucciero, Maria Teresa Terracciano, Sarmad Shakeel, Vincenzo Macillo, Ornella Iuorio, and Luigi Fiorino. 2019. "Seismic Response Assessment of Architectural Non-Structural LWS Drywall Components through Experimental Tests." Journal of Constructional Steel Research 162:105575. https://doi.org/10.1016/j.jcsr.2019.04.011.
- Santos, Ana Francisca, Aldina Santiago, Massimo Latour, Gianvittorio Rizzano, and Luís Simões da Silva. 2020. "Response of Friction Joints under Different Velocity Rates." *Journal of Constructional Steel Research* 168:106004. https://doi.org/10.1016/j.jcsr.2020.106004.